ous medium through supramolecular assembly. *Macromolecules.* **29**:6183–6188 (1996) doi:10.1021/ma960487p.

25. A. Harada, and K. Kataoka. Formation of polyion complex micelles in an aqueous milieu from a pair of oppositely-charged block copolymers with poly(ethylene glycol) segments. *Macromolecules.* **28**:5294–5299 (1995) doi:10.1021/ma00119a019.
26. K. Itaka, K. Yamauchi, A. Harada, K. Nakamura, H. Kawaguchi, and K. Kataoka. Polyion complex micelles from plasmid DNA and poly(ethylene glycol)-poly(L-lysine) block copolymer as serum-tolerable polyplex system: physicochemical properties of micelles relevant to gene transfection efficiency. *Biomaterials.* **24**:4495–4506 (2003) doi:10.1016/S0142-9612(03)00347-8.
27. Y. Matsumura, and H. Maeda. A new concept for macromolecular therapeutics in cancer chemotherapy: mechanism of tumoritropic accumulation of proteins and the antitumor agent SMANCS. *Cancer Res.* **46**:6387–6392 (1986).

DOI: 10.1002/anie.200800963

Cell Transfection

# Charge-Conversion Ternary Polyplex with Endosome Disruption Moiety: A Technique for Efficient and Safe Gene Delivery**

*Yan Lee, Kanjiro Miyata, Makoto Oba, Takehiko Ishii, Shigeto Fukushima, Muri Han, Hiroyuki Koyama, Nobuhiro Nishiyama, and Kazunori Kataoka**

DNA or RNA delivery into target cells by synthetic nonviral vectors (lipoplexes and polyplexes) is widely recognized as a promising alternative to delivery with viral vectors, which encounter the safety issues inherent to their biological propensities.[1] Nevertheless, even in the case of nonviral vectors, the inconsistency between the delivery efficiency and the safety issue, particularly with regard to chemotoxicity, has been a major matter of concern. The vectors with high transfection efficiency often show high toxicity, whereas those with low toxicity frequently raise the issue of low transfection efficiency.

Various polycations with regulated basicity have been developed for the construction of polyplexes directed toward high transfection efficiency since Behr and co-workers introduced to the gene-delivery field the concept of endosomal escape through the "proton-sponge" effect hypothesized for polyethyleneimine (PEI), yet the toxicity of these polycations lends the polyplexes to only limited applications.[2] One of the main reasons for the limited success is probably that different, and even conflicting, functionalities of the polyplexes are required at each different stage of the delivery processes. For example, the moieties of high amine density in the polyplexes are important to overcome endosomal membrane barriers because their protonation potential contributes to endosome buffering as well as to membrane destabilization.[3] On the other hand, the positively charged nature of the polyplexes may induce nonspecific interactions with negatively charged serum components to form thrombi in the capillary and carries the risk of perturbing the structure of the plasma membrane to induce high cytotoxicity and excessive immune responses.[4] Shielding of the positive charges by covering the polyplex surface with polyanions[5] or poly(ethylene glycol) (PEG)[6] is a well-known practical solution to these problems, yet significant lowering of the transfection efficiency is inevitable, mainly due to the reduced cellular uptake and the impaired capacity for endosome escape. Therefore, much effort has been concentrated on the development of deshielding methods at a specific stage during the transfection process.[7]

Herein, we wish to communicate a novel approach to the design of polyplexes exerting both high transfection efficiency and lowered cytotoxicity by integrating a charge-conversion moiety into the polyplex structure. Maleic amide derivatives, *cis*-aconitic amide, and citraconic amide have negative charges at neutral pH values, but they degrade promptly at weakly acidic pH 5.5 to expose positively charged amines.[8] Therefore, if we cover the surface of the positively charged polyplexes with degradable amide-derivatized polymers to form ternary polyplexes (plasmid DNA/polycation/polyanion with the degradable side chain), the polyplexes maintain a neutral to negatively charged nature on the cell exterior, whereas the charge-conversion components are expected to turn positive in the acidic milieu of the endosome to facilitate the endosomal escape of the polyplexes through membrane disruption (Figure 1).

Initially, a polyplex between plasmid DNA (pDNA) and a polycation was prepared. As the polycation, we chose pAsp-(DET) (Figure 2A), which had been proven by our group to be an endosome-disrupting and membrane-destabilization moiety with lower cytotoxicity than conventional polycations, including PEI.[9] The polyplexes showed positive surface charges with a zeta potential of approximately +40 mV because of the excess amount of polycations (N (amines in pAsp(DET))/P (phosphate in pDNA) ratio of 4–8). The polyplex was then added to 1–4 molar equivalents of the charge-conversion polymer pAsp(DET-Aco) (Figure 2A) to form the ternary polyplex. The pAsp(DET-Aco) should turn into pAsp(DET), which could also disrupt the endosome efficiently, at the endosomal pH value after degradation of the *cis*-aconitic amide moieties. Each ternary polyplex at various charge ratios showed unimodal size distribution with a mean diameter of about 130 nm, as measured by dynamic light scattering (DLS), even in the presence of excess pAsp(DET-Aco). Although there is a possibility of the formation of the binary polyplex between pAsp(DET-Aco)

[*] Dr. Y. Lee, S. Fukushima, Dr. N. Nishiyama, Prof. Dr. K. Kataoka
Division of Clinical Biotechnology, Center for Disease Biology and Integrative Medicine, Graduate School of Medicine, University of Tokyo, 7-3-1 Hongo, Bunkyo-ku, Tokyo 113-0033 (Japan)
Fax: (+81) 3-5841-7139
E-mail: kataoka@bmw.t.u-tokyo.ac.jp
Dr. K. Miyata, Dr. T. Ishii, Prof. Dr. K. Kataoka
Department of Bioengineering, University of Tokyo
7-3-1 Hongo, Bunkyo-ku, Tokyo 113-0033 (Japan)
Dr. M. Oba, Prof. Dr. H. Koyama
Department of Clinical Vascular Regeneration, University of Tokyo
7-3-1 Hongo, Bunkyo-ku, Tokyo 113-0033 (Japan)
Dr. K. Miyata, Dr. N. Nishiyama, Prof. Dr. K. Kataoka
Center for Nanobio Integration, University of Tokyo
7-3-1 Hongo, Bunkyo-ku, Tokyo 113-8656 (Japan)
Dr. M. Han, Prof. Dr. K. Kataoka
Department of Materials Engineering, University of Tokyo
7-3-1 Hongo, Bunkyo-ku, Tokyo 113-8656 (Japan)

[**] This work was supported by a Core Research for Evolutional Science and Technology (CREST) grant from the Japan Science and Technology Agency (JST).

Supporting information for this article is available on the WWW under http://www.angewandte.org or from the author.


© 2008 Wiley-VCH Verlag GmbH & Co. KGaA, Weinheim

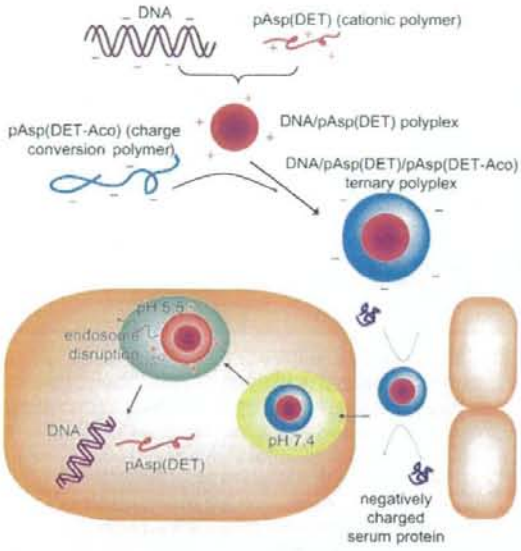


***Figure 1.*** Diagram of the charge-conversion ternary polyplex with an endosome-disrupting function. pAsp(DET): poly{*N*-[*N*'-(2-aminoethyl)-2-aminoethyl]aspartamide}; pAsp(DET-Aco): poly(*N*-{*N*'-[(*N*''-*cis*-aconityl)-2-aminoethyl]-2-aminoethyl}aspartamide).

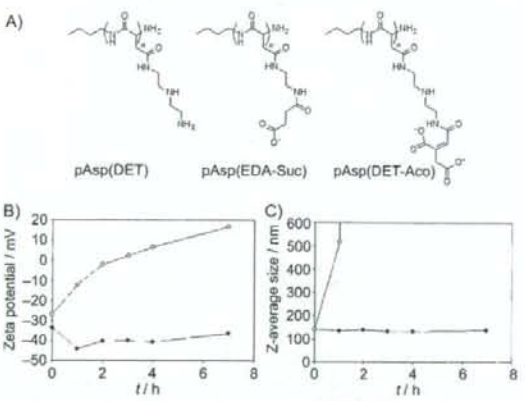


***Figure 2.*** A) The structures of the polycation pAsp(DET), the non-charge-conversion polyanion poly[(*N*'-succinyl-2-aminoethyl)aspartamide] (pAsp(EDA-Suc)), and the charge-conversion polyanion pAsp(DET-Aco). B) The charge conversion of the ternary polyplex of DNA/pAsp(DET)/pAsp(DET-Aco). C) The change of hydrodynamic diameter of the ternary polyplex. ○: results at pH 5.5; ●: results at pH 7.4.

and pAsp(DET) without DNA, the formation of the DNA-containing ternary polyplex was confirmed by gel electrophoresis assays (see the Supporting Information).

The charge-conversion behavior of the ternary polyplex was monitored from the change in the zeta potential, as illustrated in Figure 2B. The ternary polyplex maintained a zeta potential of around −40 mV at pH 7.4. However, the zeta potential at pH 5.5 increased gradually from negative to positive; this result indicates the charge conversion due to the degradation of the *cis*-aconitic amide moieties. After incubation for 2 h at pH 5.5, the zeta potential reached 0 mV. As a negative control, we used a non-charge-conversion polyanion with a similar structure, pAsp(EDA-Suc) (Figure 2A). The ternary polyplex with pAsp(DET) and pAsp(EDA-Suc) maintained a zeta potential of around −40 mV at pH 5.5 and pH 7.4, and it showed no sign of charge conversion (see the Supporting Information).

The charge conversion also induced a dramatic size change in the ternary polyplex. As shown in Figure 2C, the ternary polyplex maintained a diameter of around 130 nm at pH 7.4, but there was an immediate increase in its size at pH 5.5, even after 1 h. After 2 h, large aggregates with a diameter of over 1 μm had formed. The reason for the aggregation is probably the reduction in the repulsive forces due to the partial charge neutralization after 1 h and the complete neutralization after 2 h at pH 5.5, as indicated from the data of the zeta potential measurements.

For the potential in vivo applications, the polyplex stability in a solution of serum proteins should be addressed. In a solution of bovine serum albumin (BSA), the ternary polyplexes maintained their original diameter, whereas the positive polyplex of pAsp(DET) showed a prompt increase in diameter, even after 1 h of incubation (Figure 3A). The improved stability of the ternary polyplex was probably due to the repulsive forces between the anionic ternary polyplex and the BSA; this could be a merit for future systemic applications.

The transfection was performed by using human umbilical vein endothelial cells (HUVEC). Only limited transfection reagents have been available for these cells in the past because they are very difficult to transfect and sensitive to toxicity.[10]

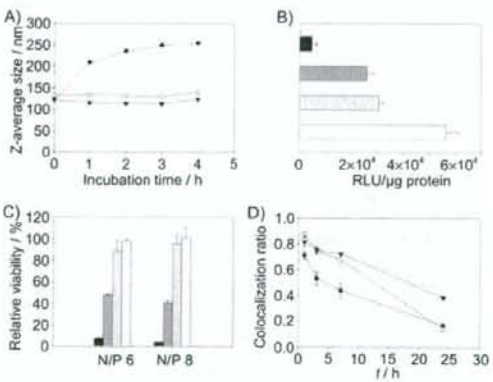


***Figure 3.*** A) The stability of the polyplex in BSA solution. B) The transfection activity of the various vectors. C) The relative viability of HUVEC transfected with the various vectors. D) The colocalization ratio of the red fluorescence of cyanine-5-labeled DNA with the green fluorescence of LysoTracker Green (see Figure 4). Error bars indicate the standard error. Black bars: ExGen 500; ● and dark gray bars: pAsp(DET) polyplex; ▼ and light gray bars: pAsp(EDA-Suc) ternary polyplex; ○ and white bars: pAsp(DET-Aco) ternary polyplex.

 © 2008 Wiley-VCH Verlag GmbH & Co. KGaA, Weinheim 

The resulting transfection data with luciferase pDNA are summarized in Figure 3B. The N/P ratios between DNA and pAsp(DET) in both the simple polyplex and the ternary polyplex were 6, the value at which they showed the highest transfection efficiency. The ternary polyplexes were formed by addition of two molar equivalents of pAsp(DET-Aco) or pAsp(EDA-Suc) to the simple polyplex. The control ternary polyplex with pAsp(EDA-Suc) showed similar transfection efficiency to the simple polyplex of pAsp(DET), whereas the charge-conversion ternary polyplex of pAsp(DET-Aco) showed a tranfection efficiency that was more than ten times higher than that of ExGen 500, a commercially available transfection reagent of linear PEI, and two times higher than that of the pAsp(DET) polyplex. Even though the negative surface charge of the ternary complex was not helpful for the cellular uptake and endosomal escape, it increased the stability of the complex in the presence of the serum proteins, as shown in Figure 3A, and reduced the toxicity, so that the non-charge-conversion ternary polyplex (DNA/pAsp(DET)/pAsp(DET-Suc)) showed similar transfection efficiency to the simple polyplex. With the introduction of the charge-conversion endosome-disrupting moiety into the ternary polyplex on the basis of that stability and low toxicity (DNA/pAsp(DET)/pAsp(DET-Aco)), the transfection efficiency was still more increased. The transfection results with yellow-fluorescence-protein (YFP) pDNA, which also showed the appreciable transfection efficiency of the ternary polyplex system, is summarized in the Supporting Information.

The cytotoxicity, as measured by an MTT viability assay, is shown in Figure 3C. At N/P ratios of 6 and 8, which were the optimal ratios for the transfection, ExGen 500 showed very high toxicity with a viability below 10%, and the pAsp(DET) polyplex also showed the viability to be decreased to 50%. One of the main reasons for the decreased viability was probably the positive surface charge of the polyplexes inducing membrane toxicity.[11] However, the ternary polyplexes, which had negatively charged surfaces at the cell exterior, showed almost no cytotoxicity at both N/P ratios.

For the confirmation of the enhanced endosomal escape of the charge-conversion ternary polyplex, the intracellular distribution of the polyplex was investigated by confocal laser scanning microscopy (CLSM) by using cyanine-5-labeled pDNA (Figure 4). The yellow fluorescence changes to red when the polyplex is released from the acidic vasicular organelles. The positively charged pAsp(DET) polyplex showed significant endosomal escape, even only after 3 h, and over 80% of the DNA had escaped after 24 h. Both ternary polyplexes showed low endosomal escape after 3 h. However, the charge-conversion ternary polyplex from pAsp(DET-Aco) showed similar levels of endosomal escape to the positive pAsp(DET) polyplex after 24 h, whereas large portions (over 40%) of the non-charge-conversion ternary polyplex with pAsp(EDA-Suc) still remained in the endosomes.

The quantitative analyses of the CLSM images are summarized in Figure 3D. The charge-conversion polyplex showed similar behavior to the non-charge-conversion polyplex until 3 h, but it showed less colocalization ratio after 7 h, and finally had a similar ratio to the positive pAsp(DET) polyplex after 24 h. By considering that the endosomal acidification and the charge conversion required some time, the CLSM data were reasonable and agreed with the luciferase transfection data.

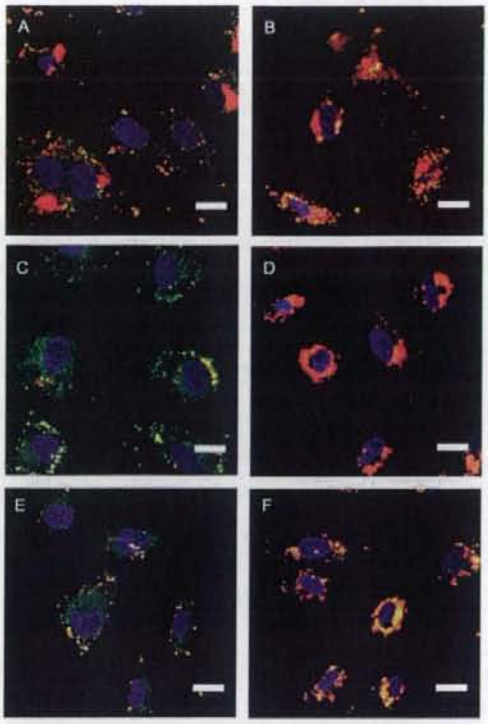


***Figure 4.*** CLSM images of HUVEC transfected with pAsp(DET) polyplex (A and B), pAsp(DET-Aco) ternary polyplex (C and D), and pAsp(EDA-Suc) ternary polyplex (E and F). (A, C, and E) are images after 3 h of transfection; (B, D, and F) are images after 24 h of transfection. Plasmid DNA labeled with cyanine 5 (red) was used. The cell nuclei were stained with Hoechst 33342 (blue), and the late endosome and lysosome were stained with LysoTracker Green (green). Each scale bar represents 20 μm.

In summary, we have developed ternary polyplexes that express negative charges at the pH value of the cell exterior and that turn positive to disrupt the endosome at endosomal pH values. Eventually, these polyplexes achieved appreciably high transfection activity and low toxicity against sensitive primary cells (HUVEC). The transfection efficiency of this ternary polyplex system could be enhanced more by the conjugation of appropriate ligands, such as an RGD peptide for active internalization through binding of the integrin receptor.[12] The concept of our charge-conversion ternary polyplex with an endosome-disrupting moiety could easily be applied to various sensitive primary cells, the efficient and non-chemotoxic transfection of which is one of the most important and urgent issues in the biomedical field. Also, the stability of the ternary polyplex in the presence of negatively


© 2008 Wiley-VCH Verlag GmbH & Co. KGaA, Weinheim

charged serum proteins could be helpful for the development of in vivo gene vectors.

Received: February 28, 2008
Revised: April 10, 2008
Published online: June 4, 2008

**Keywords:** charge conversion · DNA · gene delivery · polymers · transfection

[1] a) D. W. Pack, A. S. Hoffman, S. Pun, P. S. Stayton, *Nat. Rev. Drug Discovery* **2005**, *4*, 581–593; b) E. Mastrobattista, M. A. E. M. Aa, W. E. Hennink, D. J. A. Crommelin, *Nat. Rev. Drug Discovery* **2006**, *5*, 115–121.

[2] a) O. Boussif, F. Lezoualc'h, M. A. Zanta, M. D. Mergny, D. Scherman, B. Demeneix, J. P. Behr, *Proc. Natl. Acad. Sci. USA* **1995**, *92*, 7297–7301; b) M. Neu, D. Fischer, T. Kissel, *J. Gene Med.* **2005**, *7*, 992–1009.

[3] a) M. X. Tang, C. T. Redemann, F. C. Szoka, *Bioconjugate Chem.* **1996**, *7*, 703–714; b) R. Wattiaux, N. Laurent, S. W.-D. Coninck, M. Jadot, *Adv Drug Delivery Rev.* **2000**, *41*, 201–208.

[4] a) A. C. Hunter, *Adv. Drug Delivery Rev.* **2006**, *58*, 1523–1531; b) M. Ogris, S. Brunner, S. Schüler, R. Kircheis, E. Wagner, *Gene Ther.* **1999**, *6*, 595–605.

[5] V. S. Trubetskoy, S. C. Wong, V. Subbotin, V. G. Budker, A. Loomis, J. E. Hagstrom, J. A. Wolff, *Gene Ther.* **2003**, *10*, 261–271.

[6] M. Han, Y. Bae, N. Nishiyama, K. Miyata, M. Oba, K. Kataoka, *J. Controlled Release* **2007**, *121*, 38–48.

[7] a) E. R. Gillies, A. P. Goodwin, J. M. Fréchet, *Bioconjugate Chem.* **2004**, *15*, 1254–1263; b) M. Krämer, J. F. Stumbé, H. Türk, S. Krause, A. Komp, L. Delineau, S. Prokhorova, H. Krautz, R. Haag, *Angew. Chem.* **2002**, *114*, 4426–4431; *Angew. Chem. Int. Ed.* **2002**, *41*, 4252–4256.

[8] a) Y. Lee, S. Fukushima, Y. Bae, S. Hiki, T. Ishii, K. Kataoka, *J. Am. Chem. Soc.* **2007**, *129*, 5362–5363; b) D. B. Rozema, D. L. Lewis, D. H. Wakefield, S. C. Wong, J. J. Klein, P. L. Roesch, S. L. Bertin, T. W. Reppen, Q. Chu, A. V. Blokhin, J. E. Hagstrom, J. A. Wolff, *Proc. Natl. Acad. Sci. USA* **2007**, *104*, 12982–12987.

[9] a) N. Kanayama, S. Fukushima, N. Nishiyama, K. Itaka, W.-D. Jang, K. Miyata, Y. Yamasaki, U.-I. Chung, K. Kataoka, *ChemMedChem* **2006**, *1*, 439–444; b) K. Masago, K. Itaka, N. Nishiyama, U. Chung, K. Kataoka, *Biomaterials* **2007**, *28*, 5169–5175.

[10] a) V. Zaric, D. Weltin, P. Erbacher, J. S. Remy, J. P. Behr, D. Stephan, *J. Gene Med.* **2004**, *6*, 176–184; b) J. J. Green, G. T. Zugates, N. C. Tedford, Y. H. Huang, L. G. Griffith, D. A. Lauffenburger, J. A. Sawicki, R. Langer, D. G. Anderson, *Adv. Mater.* **2007**, *19*, 2836–2842.

[11] a) D. Fischer, Y. Li, B. Ahlemeyer, J. Krieglstein, T. Kissel, *Biomaterials* **2003**, *24*, 1121–1131; b) S. M. Moghimi, P. Symonds, J. C. Murray, A. C. Hunter, G. Debska, A. Szewczyk, *Mol. Ther.* **2005**, *11*, 990–995.

[12] a) K. Temming, R. M. Schiffelers, G. Molema, R. J. Kok, *Drug Resist. Updates* **2005**, *8*, 381–402; b) M. Oba, S. Fukushima, N. Kanayama, K. Aoyagi, N. Nishiyama, H. Koyama, K. Kataoka, *Bioconjugate Chem.* **2007**, *18*, 1415–1423.

 © 2008 Wiley-VCH Verlag GmbH & Co. KGaA, Weinheim 

J|A|C|S
ARTICLES

Published on Web 04/09/2008

# PEG-Detachable Polyplex Micelles Based on Disulfide-Linked Block Catiomers as Bioresponsive Nonviral Gene Vectors

Seiji Takae,[†] Kanjiro Miyata,[‡,⊥] Makoto Oba,[§] Takehiko Ishii,[‡,⊥] Nobuhiro Nishiyama,[∥,⊥] Keiji Itaka,[∥] Yuichi Yamasaki,[†,⊥] Hiroyuki Koyama,[§] and Kazunori Kataoka*[,†,‡,∥,⊥]

*Department of Materials Engineering, Graduate School of Engineering, The University of Tokyo, 7-3-1 Hongo, Bunkyo-ku, Tokyo 113-8656, Japan, Department of Bioengineering, Graduate School of Engineering, The University of Tokyo, 7-3-1 Hongo, Bunkyo-ku, Tokyo 113-8656, Japan, Department of Clinical Vascular Regeneration, Graduate School of Medicine, The University of Tokyo, 7-3-1 Hongo, Bunkyo-ku, Tokyo 113-8655, Japan, Division of Clinical Biotechnology, Center for Disease Biology and Integrative Medicine, Graduate School of Medicine, The University of Tokyo, 7-3-1 Hongo, Bunkyo-ku, Tokyo 113-0033, Japan, and Center for NanoBio Integration, The University of Tokyo, 7-3-1 Hongo, Bunkyo-ku, Tokyo 113-8656, Japan*

Received January 15, 2008; E-mail: Kataoka@bmw.t.u-tokyo.ac.jp

***Abstract:*** PEG-based polyplex micelles, which can detach the surrounding PEG chains responsive to the intracellular reducing environment, were developed as nonviral gene vectors. A novel block catiomer, PEG-SS-P[Asp(DET)], was designed as follows: (i) insertion of biocleavable disulfide linkage between PEG and polycation segment to trigger PEG detachment and (ii) a cationic segment based on poly(aspartamide) with a flanking *N*-(2-aminoethyl)-2-aminoethyl group, P[Asp(DET)], in which the Asp(DET) unit acts as a buffering moiety inducing endosomal escape with minimal cytotoxicity. The polyplex micelles from PEG-SS-P[Asp(DET)] and plasmid DNA (pDNA) stably dispersed in an aqueous medium with a narrowly distributed size range of ~80 nm due to the formation of hydrophilic PEG palisades while undergoing aggregation by the addition of 10 mM dithiothreitol (DTT) at the stoichiometric charge ratio, indicating the PEG detachment from the micelles through the disulfide cleavage. The PEG-SS-P[Asp(DET)] micelles showed both a 1–3 orders of magnitude higher gene transfection efficiency and a more rapid onset of gene expression than PEG-P[Asp(DET)] micelles without disulfide linkages, due to much more effective endosomal escape based on the PEG detachment in endosome. These findings suggest that the PEG-SS-P[Asp(DET)] micelle may have promising potential as a nonviral gene vector exerting high transfection with regulated timing and minimal cytotoxicity.

## Introduction

Successful gene therapy, which is a promising treatment for numerous intractable diseases, relies on the development of efficient gene vectors. Polyplexes formed by electrostatic interaction between plasmid DNA (pDNA) and cationic polymers (catiomers) have attracted much attention as a safe, versatile alternative to viral vectors.[1-7] A promising approach to realizing the polyplexes for in vivo gene delivery is the use of PEG-based block catiomers. These catiomers spontaneously associate with pDNA to form sub-100 nm polyplex micelles with a dense, hydrophilic PEG palisade surrounding the core.[8-11] These micelles show high colloidal stability under physiological conditions and substantial transfection activity against various cell types even after preincubation with serum proteins.[12,13] Moreover, polyplex micelles demonstrate prolonged blood circulation and in vivo gene transfer to the liver and tumor.[14-16]

[†] Department of Materials Engineering, The University of Tokyo.
[‡] Department of Bioengineering, The University of Tokyo.
[§] Department of Clinical Vascular Regeneration, The University of Tokyo.
[∥] Center for Disease Biology and Integrative Medicine, The University of Tokyo.
[⊥] Center for NanoBio Integration, The University of Tokyo.

(1) Pack, D. W.; Hoffman, A. S.; Pun, S.; Stayton, P. S. *Nat. Rev. Drug Discov.* **2005**, *4*, 581–593.
(2) Merdan, T.; Kopecek, J.; Kissel, T. *Adv. Drug Delivery Rev.* **2002**, *54*, 715–758.
(3) Wagner, E.; Meyer, M. *Hum. Gene Ther.* **2006**, *17*, 1062–1076.
(4) Kabanov, A. V. *Adv. Drug Delivery Rev.* **2006**, *58*, 1597–1621.
(5) Park, T. G.; Jeong, J. H.; Kim, S. W. *Adv. Drug Delivery Rev.* **2006**, *58*, 467–486.
(6) Osada, K.; Kataoka, K. *Adv. Polym. Sci.* **2006**, *202*, 113–153.
(7) Neu, M.; Fischer, D.; Kissel, T. *J. Gene Med.* **2005**, *7*, 992–1009.
(8) Katayose, S.; Kataoka, K. *Bioconjugate Chem.* **1997**, *8*, 702–707.
(9) Katayose, S.; Kataoka, K. *J. Pharm. Sci.* **1998**, *87*, 160–163.
(10) Ogris, M.; Brunner, S.; Schuller, S.; Kircheis, S.; Wagner, E. *Gene Ther.* **1999**, *6*, 595–605.
(11) Kwok, K. Y.; McKenzie, D. L.; Evers, D. L.; Rice, K. G. *J. Pharm. Sci.* **1999**, *88*, 996–1003.
(12) Itaka, K.; Yamauchi, K.; Harada, A.; Nakamura, K.; Kawaguchi, H.; Kataoka, K. *Biomaterials* **2003**, *24*, 4495–4506.
(13) Itaka, K.; Harada, A.; Nakamura, K.; Kawaguchi, H.; Kataoka, K. *Biomacromolecules* **2002**, *3*, 841–845.
(14) Harada-Shiba, M.; Yamauchi, K.; Harada, A.; Takanisawa, I.; Shimokado, K.; Kataoka, K. *Gene Ther.* **2002**, *9*, 407–414.
(15) Miyata, K.; Kakizawa, K.; Nishiyama, N.; Yamasaki, Y.; Watanabe, T.; Kohara, M.; Kataoka, K. *J. Controlled Release* **2005**, *109*, 15–23.

10.1021/ja800336v CCC: $40.75 © 2008 American Chemical Society

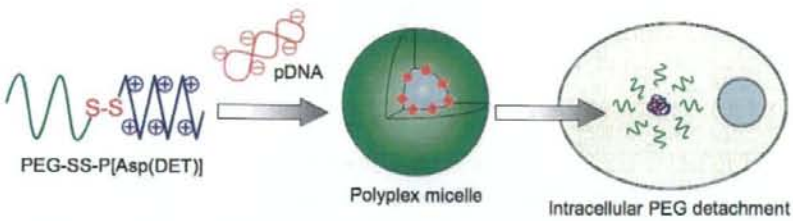


***Figure 1.*** Schematic illustration of PEG-detachable polyplex micelle formation and the PEG detachment in the reducing intracellular environment.

We recently reported high transfection efficiency and low cytotoxicity with the use of polyplex micelles formed by PEG-*block*-poly(aspartamide) copolymers carrying the *N*-(2-aminoethyl)-2-aminoethyl group in the side chain (PEG-P[Asp(DET)]).[17] With regard to in vivo application, the polyplex micelles demonstrate appreciable gene transfer into vascular lesions without any vessel occlusion by thrombus[18] and bone regeneration of a mouse bone defect when transfected with genes coding for osteogenic factors.[19] These successful in vivo gene therapies have been explained by the specific structure of the side chain of P[Asp(DET)], in which the 1,2-ethanediamine moiety of the *N*-(2-aminoethyl)-2-aminoethyl group exhibits a distinct two-step protonation behavior, suggesting a potential proton sponge capacity of Asp(DET) units for efficient endo/lysosomal escape.[17]

However, polyplex micelles formed from PEG-P[Asp(DET)] could be further improved upon to achieve successful in vivo systemic therapies. P[Asp(DET)] homopolymer polyplexes show higher transfection efficiency than PEG-P[Asp(DET)] micelles especially at low charge ratios,[20] suggesting that the PEG palisade surrounding PEG-P[Asp(DET)] polyplex micelles would hamper the transfection. The decrease in gene transfection efficiency by PEGylation to cationers (PEG dilemma) is also observed in previous work.[16,21,22] In addition, the time-dependent monitoring of gene expression against multicellular tumor spheroids reveals that the polyplex micelles from PEG-P[Asp(DET)] cause delayed gene expression, compared with polyplexes from cationic homopolymers.[20] This is sometimes undesired especially when rapid expression is required. On the other hand, the polyplexes from P[Asp(DET)] homocationers tend to aggregate through interactions with serum proteins,[18] suggesting limited in vivo application of the system without PEGylation. Although P[Asp(DET)] homocationers exhibited appreciably lower cytotoxicity compared with typical polycations such as polyethyleneimine (PEI),[23] PEGylation to P[Asp(DET)] further decreases the cytotoxicity to obtain successful transfection of primary cells.[17,18,20]

In order to overcome the aforementioned PEG dilemma, we designed here PEG detachable smart polyplex micelles sensitive to the intracellular environment as a smart gene vector (Figure 1). Block cationers containing disulfide linkages between PEG and P[Asp(DET)] segments, PEG-SS-P[Asp(DET)], were synthesized to obtain this design goal (Scheme 1). Subsequent disulfide reduction of the block cationer can occur during several steps of the endocytic pathway.[24] The cytoplasm and nuclear space are highly reducing environments due to abundant reduced glutathione (GSH) as well as redox enzymes such as the thioredoxin family. In addition, several studies suggest that disulfide bond reduction can begin on the exofacial surface of the cell and must continue after endocytosis. In this regard, involvement of plasma membrane-associated protein disulfide isomerase (PDI) is strongly implicated, as disulfide reduction is inhibited by an anti-PDI antibody and a PDI-inhibitor.[25,26] Moreover, NADH-oxidase (NOX) is reported as another cell surface-associated protein with disulfide−thiol interchange activity similar to PDI. Interestingly, the activity of this enzyme is constitutively activated in cancerous cells such as HeLa and hepatoma cells.[27] Finally, cysteine is actively transported from the cytoplasm to the lysosome lumen via a specific transporter in fibroblasts.[28]

Though the cleavage mechanism of the disulfide linkages cannot be predicted for the PEG-SS-P[Asp(DET)] micelle system utilized herein, the effect of PEG detachment on the gene transfection efficiency can be predicted based on where cleavage may occur. As a result of PEG detachment at the cell surface, the exposed cation segments may trigger a strong association to cells, increasing the cellular uptake of the micelles. Inside endosomes, the PEG detachment would cause the interaction between the exposed cation segments and the endosomal membrane and/or increase endosomal pressure, resulting in the destruction of the endosomal membrane to enable effective endosomal escape. In the cytoplasm and nucleus, the release of pDNA that forms the polyplex core might become smoother because steric repulsion disappears as the PEG cleaves, causing easier access of cellular polyanions to the complex core. Even if the reduction of disulfide linkages occurs in any of the steps outlined above, a more rapid alteration of gene expression and an increased transfection efficiency are expected.

(16) Kursa, M.; Walker, G. F.; Roessler, V.; Ogris, M.; Roedl, W.; Kircheis, R.; Wagner, E. *Bioconjugate Chem.* **2003**, *14*, 222–231.
(17) Kanayama, N.; Fukushima, S.; Nishiyama, N.; Itaka, K.; Jang, W.-D.; Miyata, K.; Yamasaki, Y.; Chung, U.-i.; Kataoka, K. *ChemMedChem* **2006**, *1*, 439–444.
(18) Akagi, D.; Oba, M.; Koyama, H.; Nishiyama, N.; Fukushima, S.; Miyata, T.; Nagawa, H.; Kataoka, K. *Gene Ther.* **2007**, *14*, 1029–1038.
(19) Itaka, K.; Ohba, S.; Miyata, K.; Kawaguchi, H.; Nakamura, K.; Takato, T.; Chung, U.-i.; Kataoka, K. *Mol. Ther.* **2007**, *15*, 1655–1662.
(20) Han, M.; Bae, Y.; Nishiyama, N.; Miyata, K.; Oba, M.; Kataoka, K. *J. Controlled Release* **2007**, *121*, 38–48.
(21) Brissault, B.; Kichler, A.; Leborgne, C.; Danos, O.; Cheradame, H.; Gau, J.; Auvray, L.; Guis, C. *Biomacromolecules* **2006**, *7*, 2863–2870.
(22) Sagara, K.; Kim, S. W. *J. Controlled Release* **2002**, *79*, 271–281.
(23) Masago, K.; Itaka, K.; Nishiyama, N.; Chung, U.-i.; Kataoka, K. *Biomaterials* **2007**, *28*, 5169–5175.
(24) Saito, G.; Swanson, J. A.; Lee, K.-D. *Adv. Drug Delivery Rev.* **2003**, *55*, 199–215.
(25) Feener, E. P.; Shen, W. C.; Ryser, H. J. *J. Biol. Chem.* **1990**, *265*, 18780–18785.
(26) Mandel, R.; Ryser, H. J.; Ghani, F.; Wu, M.; Peak, D. *Proc. Natl. Acad. Sci. U.S.A.* **1993**, *90*, 4112–4116.
(27) Morre, D. J.; Morre, D. M. *Free Radical Res.* **2003**, *37*, 795–808.
(28) Pisoni, R. L.; Acker, T. L.; Lisowski, K. M.; Lemons, R. M.; Thoene, J. G. *J. Cell Biol.* **1990**, *110*, 327–335.

**Scheme 1.** Synthetic Route of PEG-SS-P[Asp(DET)] Synthesis (Left) and the Chemical Structures of Control Polymers Used in This Experiment (PEG-P[Asp(DET)] and P[Asp(DET)]) (Right)

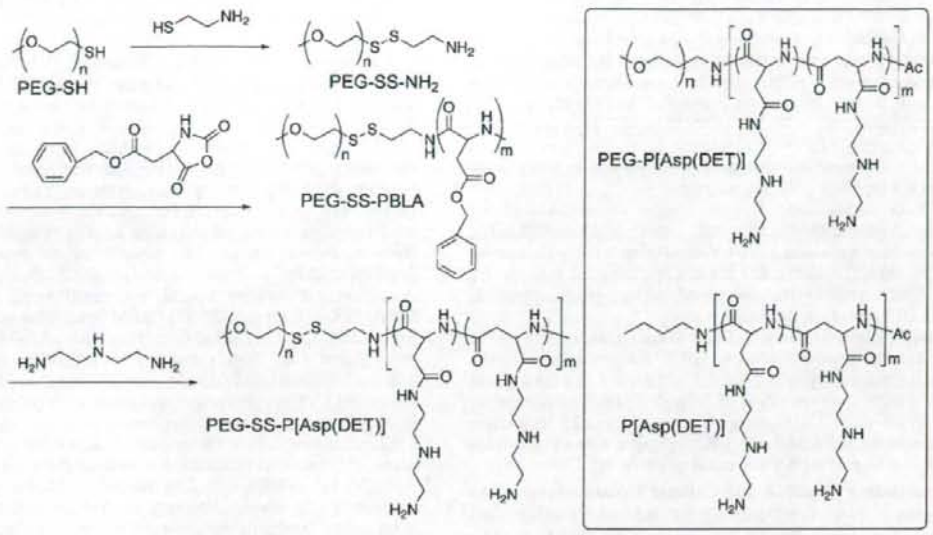


Based on such assumptions, we newly synthesized the PEG-SS-P[Asp(DET)] copolymer and prepared polyplex micelles sensitive to reducing environments. These micelles were expected to show comparable colloidal stability to PEG-P[Asp(DET)] micelles before cellular uptake, while, inside the cell, detachment of PEG would enable pDNA activity and alteration to gene expression. Therefore, careful characterization of both the PEG-SS-P[Asp(DET)] copolymer and the polyplex micelles was performed in regards to the reduction of disulfide linkages. In addition, the influence of the PEG detachment on the onset of gene expression and the mechanism of the disulfide reduction were evaluated through the time-dependent observation of the gene expression and the intracellular localization of pDNA.

## Materials and Methods

**Materials.** α-Methoxy-ω-mercapto PEG (PEG-SH, $M_n = 10000$, $M_w/M_n = 1.03$) and β-benzyl-L-aspartate *N*-carboxyanhydride (BLA-NCA) were obtained from NOF Co. (Tokyo, Japan). Methanol (MeOH), 2-aminoethanethiol, benzene, acetonitrile, hexane, ethyl acetate, and D-luciferin were purchased from Wako Chemical Industries, Ltd. (Osaka, Japan). Dichloromethane, *N*,*N*-dimethylformamide (DMF), diethylenetriamine (DET), and *N*-methyl-2-pyrrolidone (NMP) were also purchased from Wako Chemical Industries and purified by distillation before use. A pGL3 control vector, which was purchased from Promega Co. (Madison, WI), was used as pDNA in all the experiments. This pDNA was amplified in competent DH5α *Escherichia coli* and purified using HiSpeed Plasmid MaxiKit purchased from QIAGEN Inc. (Valencia, CA). Water was purified using a Milli-Q instrument (Millipore, Bedford, MA).

**Synthesis of PEG-SS-P[Asp(DET)].** As shown in Scheme 1, PEG-SH (1 g, 0.1 mmol) was dissolved in MeOH (100 mL), followed by the reaction with 2-aminoethanethiol (100 equiv to PEG-SH, 0.77 g, 10 mmol) at room temperature to obtain PEG-SS-$NH_2$. After a GPC peak due to PEG dimers (PEG-SS-PEG) generated by the side reaction disappeared, the reaction mixture was dialyzed against MeOH for 2 days and evaporated. Then, 80 mL of benzene were added, and the mixture was freeze-dried to obtain the white powder. To remove the PEG disulfide dimers (PEG-SS-PEG) generated during the dialysis, the powder dissolved in 30 mL of $H_2O/CH_3CN$ (4:1) was loaded onto a CM Sephadex C-50 cation exchange chromatograph (GE Healthcare UK, Ltd., Little Chalf-ont, England), eluted with $H_2O/CH_3CN$ (4:1) containing 0.125% $NH_3$. The eluate was evaporated and freeze-dried with distilled water to obtain the PEG-SS-$NH_2$ (570 mg, 57% yield). From gel permeation chromatography (GPC), $M_n$ and $M_w/M_n$ were determined to be 9880 and 1.02, respectively. The conversion to the aminoethanethiol moiety was confirmed to be quantitative (94%) based on the $^1$H NMR data [$CH_3$ (3.2 ppm) and $CH_2$ (2.8 ppm)] (Figure S1) measured with a JEOL EX300 spectrometer (JEOL, Tokyo, Japan).

The PEG-SS-poly(β-benzyl L-aspartate) (PEG-SS-PBLA) copolymer was prepared by the ring opening polymerization of BLA-NCA (4.4 mmol, 1.1 g) in $CH_2Cl_2$/DMF (10:1, 15 mL) at 35 °C from the terminal primary amino group of PEG-SS-$NH_2$ (0.04 mmol, 400 mg).[29] The reaction mixture was precipitated into hexane/AcOEt (6:4). After filtration, the precipitate was dissolved in a small amount of $CH_2Cl_2$, followed by the addition of an excess amount of benzene, and lyophilized to obtain the white powder (910 mg, 61% yield). The degree of polymerization (DP) of PBLA was calculated to be 100 from $^1$H NMR spectroscopy based on the peak intensity of benzyl protons of PBLA side chains (7.3 ppm) to the methylene protons of the PEG chain (3.6 ppm) (Figure S2).

Lyophilized PEG-SS-PBLA (130 mg) was dissolved in NMP (5.2 mL) at 27 °C, followed by the reaction with DET (2.3 mL, 50 equiv to benzyl group of PBLA segment) diluted in NMP (2.3 mL) under anhydrous conditions at 15 °C. After 15 min, the reaction mixture was slowly added dropwise into an aqueous solution of acetic acid (10% v/v, 40 mL) and dialyzed against a solution of 0.01 N HCl and, subsequently, distilled water (MWCO: 6–8000 Da). The final solution was lyophilized to obtain the polymer as the chloride salt form with a yield of 66% (104 mg). The structure of this block cationer was confirmed by $^1$H NMR and size-exclusion chromatography (SEC) [column: Superdex 200 10/300 GL (GE Healthcare UK, Ltd.); eluent: 10 mM Tris-HCl buffer + 500 mM NaCl (pH 7.4); flow rate: 0.75 mL/min; detector RI; ambient temperature].

(29) Harada, A.; Kataoka, K. *Macromolecules* **1995**, *28*, 5294–5299.

**Preparation of PEG-SS-P[Asp(DET)]/pDNA Polyplex Micelles.** The PEG-SS-P[Asp(DET)] block copolymer and pDNA were separately dissolved in 10 mM Tris-HCl buffer (pH 7.4). The polymer solution was added to a 2-times-excess volume of 50 $\mu$g/mL pDNA solution to form the polyplex micelles at various *N/P*, the residual molar ratio of the amino group in the block catiomer to phosphate group in pDNA. The final concentration of pDNA in all the samples was adjusted to 33 $\mu$g/mL. The PEG-P[Asp(DET)] block copolymer ($M_w$ = 39 000; DP of P[Asp(DET)] segment: 100) and P[Asp(DET)] (DP = 98) (Scheme 1) were used as controls, and their polyplexes were prepared in the same way as PEG-SS-P[Asp(DET)]/pDNA polyplex micelles.

**Gel Retardation Assay.** Polyplex solutions formed with pDNA (33 $\mu$g/mL) were diluted to 20 $\mu$g/mL with 10 mM Tris-HCl buffer and then electrophoresed at 100 V for 1 h on a 0.9 wt% agarose gel in 3.3 mM Tris-acetic acid buffer containing 1.7 mM sodium acetate. The migrated pDNA was visualized with ethidium bromide staining (0.5 $\mu$g/mL in deionized water).

**Dynamic Light Scattering (DLS) Measurements.** The size of the polyplexes was evaluated by DLS. Sample solutions with various *N/P* ratios in 10 mM Tris-HCl buffer (pH 7.4) were adjusted to have a pDNA concentration of 33 $\mu$g/mL. DLS measurements were carried out at 37 °C using a Zetasizer Nano-ZS instrument (Malvern Instruments, Malvern, UK), equipped with a He−Ne ion laser ($\lambda$ = 633 nm) with a scattering angle of 90°.

**Radiolabeling of pDNA and Cellular Uptake Study of the Polyplexes.** pDNA was radioactively labeled with $^{32}$P-dCTP using the Nick Translation System (Invitrogen Co., Carlsbad, CA). Unincorporated nucleotides were removed using the High Pure PCR Product Purification Kit (Roche Diagnostics Co., Indianapolis, IN). After the purification, 7 $\mu$g of labeled pDNA were mixed with 700 $\mu$g of nonlabeled pDNA. The polyplex and micelle samples were prepared by mixing the radioactive pDNA solution with each polymer solution (33 $\mu$g pDNA/mL). For the cellular uptake experiment, HeLa cells were seeded in Dulbecco's modified Eagle medium (DMEM) containing 10% fetal bovine serum (FBS) on 24-well tissue culture treated plates 24 h prior to experimentation. The cells were incubated with 30 $\mu$L of the radioactive polyplex solution (1 $\mu$g of pDNA/well) in 400 $\mu$L of DMEM containing 10% FBS. After 6 h of incubation, the cells were washed 3 times with PBS and lysed with 200 $\mu$L of cell culture lysis buffer (Promega, Co., Madison, WI). The lysates were mixed with 5 mL of scintillation cocktail, Ultima Gold (PerkinElmer, MA), and then, the radioactivity was measured using a liquid scintillation counter. The results are presented as a mean and standard deviation of the mean obtained from four samples.

**In Vitro Transfection.** HeLa cells were seeded on 24-well culture plates and incubated for 24 h in 400 $\mu$L of DMEM containing 10% FBS before transfection. The cells were then incubated with the polyplex micelles prepared from PEG-SS-P[Asp(DET)], PEG-P[Asp(DET)], and P[Asp(DET)] (30 $\mu$L, 1 $\mu$g of pDNA/well) with various *N/P* ratios in DMEM containing 10% FBS for 6 h, followed by an additional incubation for 42 h in the absence of polyplexes. The cells were washed in triplicate with 200 $\mu$L of Dulbecco's PBS and lysed by the addition of 400 $\mu$L/well of the Promega lysis buffer. Luciferase gene expression was evaluated using the Luciferase Assay System (Promega Co., Madison, WI) and a Lumat LB957 luminometer (Berthold Technologies Co., Bad Wildbad, Germany). The results were expressed as light units per milligram of cell protein determined by a BCA assay kit (PIERCE Biotechnology, Rockford, IL). The results are presented as a mean and standard deviation of the mean obtained from four samples.

**Time-Dependent Monitoring of in Vitro Transfection.** HeLa cells and 293T cells were seeded on 35-mm culture dishes and incubated for 24 h in 2 mL of DMEM containing 10% FBS before transfection. The cells were then incubated with the polyplex micelles prepared from PEG-SS-P[Asp(DET)], PEG-P[Asp(DET)], and P[Asp(DET)] (90 $\mu$L/dish, 3 $\mu$g of pDNA/dish) at *N/P* = 32 in DMEM containing 10% FBS. After 6 h, the medium was exchanged with fresh media containing 100 $\mu$M D-luciferin. The dishes were set in a luminometer incorporated in a small $CO_2$ incubator (AB-2550 Kronos Dio, ATTO Co., Tokyo, Japan), and the bioluminescence was monitored every 20 min (2 min collection time).

**Confocal Laser Scanning Microscope (CLSM) Observation.** pDNA was labeled with Cy5 using the Label IT Nucleic Acid Labeling Kit (Mirus, Madison, WI) according to the manufacture's protocol. HeLa cells were seeded on a 35-mm glass base dish (Iwaki, Japan) and incubated overnight in 1 mL of DMEM containing 10% FBS. After the medium was replaced with fresh medium, 90 $\mu$L of polyplex solution containing 3 $\mu$g of Cy5-labeled pDNA (*N/P* = 32) were applied. After 6 h of incubation, the medium was removed, the cells were washed twice with PBS, and fresh media was added. The intracellular distributions of the polyplex micelles were observed by CLSM following acidic late endosome and lysosome staining with LysoTracker Green (Molecular Probes, Eugene, OR). The CLSM observation was performed using LSM 510 (Carl Zeiss, Germany) with a 63× objective (C-Apochromat, Carl Zeiss, Germany) at excitation wavelengths of 488 nm (Ar laser) and 633 nm (He−Ne laser) for LysoTracker Green and Cy5, respectively. Colocalization of polyplex micelles in the late endosome and lysosome was quantified as follows:

Colocalization ratio = Cy5 pixels colocalization/Cy5 pixels total

where Cy5 pixels colocalization represents the number of pixels with Cy5 colocalizing with LysoTracker inside the cells and the Cy5 pixels total represents number of all pixels with Cy5 existing in the cells. The results are presented as a mean and standard error of the mean obtained from 10 cells.

## Results and Discussion

**Synthesis of PEG-SS-P[Asp(DET)].** A PEG-poly(aspartamide) block copolymer with a disulfide linkage between PEG and poly(aspartamide) was prepared as shown in Scheme 1. Initially, α-methoxy-ω-mercapto PEG (PEG-SH, $M_n$ = 10 000) was reacted with 2-aminothanethiol in MeOH to introduce a primary amino group into PEG-SH via a disulfide linkage. The conversion ratio was confirmed to be 94% based on the $^1$H NMR data (Figure S1). Then, β-benzyl L-aspartate *N*-carboxyanhydride (BLA-NCA) was polymerized in $CH_2Cl_2$/DMF at 35 °C by an initiation from the terminal primary amino group of PEG-SS-$NH_2$. The degree of polymerization (DP) of PBLA was calculated to be 100 from $^1$H NMR spectroscopy, and GPC measurement revealed that the obtained PEG-SS-PBLA showed a unimodal molecular weight distribution (Figure S2). The aminolysis of PEG-SS-PBLA in NMP in the presence of a molar excess of diethylenetriamine (DET, 50 equiv relative to benzyl groups) was carried out. The $^1$H NMR spectrum of the obtained polymer (Figure S3) reveals that the introduction of DET into the side chains of PBLA was almost quantitative (98.5%) in spite of the extremely short reaction time (15 min) and relatively low temperature (15 °C). The detailed mechanism of this unique aminolysis reaction of PBLA was reported elsewhere.[30] Size-exclusion chromatography (SEC) measurements revealed a unimodal molecular weight distribution of the obtained polymer (Figure 2, line 1), suggesting a minimal occurrence of inter- or intrapolymer cross-linking by DET during aminolysis. To confirm the presence of disulfide linkages between PEG and polycation segments, SEC measurement was done after the addition of 10 mM dithiothreitol (DTT) to the PEG-SS-P[Asp(DET)] solution. In the SEC chromatogram, two overlapping peaks (Figure 2, line 2) were observed at elution times extremely similar to those for PEG-SH (Figure 2, line 3) and

(30) Nakanishi, M.; Park, J.-S.; Jang, W.-D.; Oba, M.; Kataoka, K. *React. Funct. Polym.* **2007**, *67*, 1361–1372.

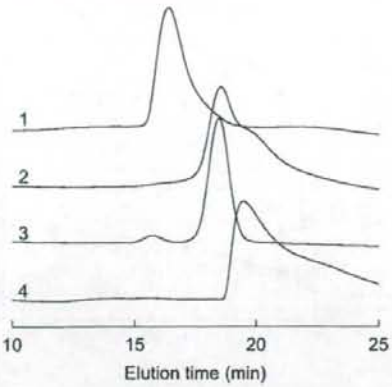


*Figure 2.* SEC charts of PEG-SS-P[Asp(DET)] (line 1), PEG-SS-P[Asp(DET)] after 4 h incubation with 10 mM DTT (line 2), PEG-SH (line 3), and P[Asp(DET)] (line 4).

P[Asp(DET)] (Figure 2, line 4), indicating that the obtained polymer was linked via a disulfide linkage between PEG and P[Asp(DET)] segments.

**Formation of Polyplex Micelles from pDNA and PEG-SS-P[Asp(DET)].** Polyplex micelles were prepared by mixing each polymer solution with the pDNA solution at various *N/P* ratios. In order to demonstrate polyplex formation between PEG-SS-P[Asp(DET)] and pDNA, a gel electrophoresis retardation assay was performed using 0.9 wt % agarose gel. A PEG-P[Asp(DET)] block copolymer without the disulfide linkage and P[Asp(DET)] homocatiomer were used as controls (Scheme 1). As shown in Figure 3, the band of free pDNA disappeared at $N/P > 2$ in all of the samples, indicating successful and complete polyplex formation between pDNA and the three catiomers. This is stoichiometrically consistent with the monoprotonated form of the ethylenediamine unit in PEG-P[Asp(DET)] and P[Asp(DET)] at pH 7.4.[17,20] The diameters of the polyplexes or the polyplex micelles prepared at different *N/P* ratios are shown in Figure 4a. The diameters of the polyplex micelles from PEG-P[Asp(DET)] and PEG-SS-P[Asp(DET)] were determined to be 80–90 nm throughout the examined *N/P* ratios (1–16). On the other hand, the polyplexes from P[Asp(DET)] formed large aggregates with a size of approximately 600 nm specifically at *N/P* ~2. Considering that zeta-potential of the P[Asp(DET)] polyplex was close to neutral at $N/P = 2$ (Figure S4), the aggregation was presumably due to the formation of charge stoichiometric complexes showing lower electrostatic repulsion among the polyplexes. The system of PEG-SS-P[Asp(DET)] and PEG-P[Asp(DET)] did not show such aggregation, indicating a high colloidal stability due to the steric repulsion of the PEG palisades of the shell.[31]

**Reducing Environment-Sensitive Cleavage of the Disulfide Linkages of the Polyplex Micelles from PEG-SS-P[Asp(DET)].** To confirm the detachment of PEG from the PEG-SS-P[Asp(DET)] polyplex micelles, the diameter of the micelles ($N/P = 2$) was monitored after the addition of 10 mM DTT, as a model reaction for the reducing environment of the cytoplasm. As shown in Figure 4b, 10 mM DTT rapidly induced an increase in size of PEG-SS-P[Asp(DET)] micelles, whereas, in the case of control

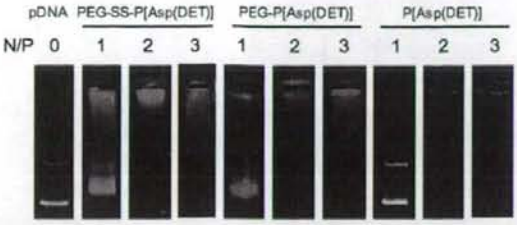


*Figure 3.* Gel retardation assay of the polyplexes.

micelles from PEG-P[Asp(DET)], such a size increase was not observed, indicating that the PEG chains on the PEG-SS-P[Asp(DET)] micelles were detached due to the cleavage of the disulfide bond. Moreover, as a model of the extracellular environment, the polyplex micelles were incubated in 10 $\mu$M DTT, which is an effective 50-fold molar equivalent of the PEG-SS-P[Asp(DET)] within the micelles. As a result, the polyplex micelles did not show increased size (Figure 4b), indicating that the PEG detachment would be dependent on the concentration of the surrounding thiol groups. To check the PEG detachment at other *N/P* ratios, the $\zeta$-potential of the polyplex micelles was measured in the absence or presence of 10 mM DTT. The polyplexes from PEG-SS-P[Asp(DET)] and PEG-P[Asp(DET)] were observed to have $\zeta$-potentials with a very small absolute value (~4 mV) in $N/P > 2$ (Figure S4), suggesting that the polyplexes from the PEG-*b*-catiomers form a core–shell micellar architecture with a hydrophilic and neutral PEG shell surrounding the polyplex core. After the addition of 10 mM DTT, the $\zeta$-potential of PEG-SS-P[Asp(DET)] polyplex micelles shifted to a positive value (~28 mV) comparable to that of the P[Asp(DET)] polyplexes. On the other hand, there was no change in the $\zeta$-potential of PEG-P[Asp(DET)] micelles by the addition of DTT. These results indicate that, regardless of *N/P* ratio, the surface-covered PEG chains detached from the PEG-SS-P[Asp(DET)] polyplex micelles when present in a reducing environment.

**Cellular Uptake Study.** Though the PEG-SS-P[Asp(DET)] polyplex micelles were responsive to reducing environments, it is significant to determine where the PEG chains will be detached after contact with cells. Rice et al. concluded that the complexes formed from PEG(5 kDa)-SS-$Lys_{18}$ and pDNA showed more in vitro cellular uptake than PEG-$Lys_{18}$ complexes without disulfide linkages, suggesting partial reduction of the disulfide linkages outside cells.[32] To confirm that the disulfide linkages were cleaved either outside or inside cells, polyplexes with $^{32}$P-radiolabeled pDNA were prepared and the uptake to human cervical carcinoma HeLa cells was measured. As shown in Figure 5, PEG-SS-P[Asp(DET)] and PEG-P[Asp(DET)] polyplex micelles showed a minimal uptake into the cells, with only ~0.5% of the total dose being taken up. In contrast, 2−4% of P[Asp(DET)] polyplexes were taken into the cells, probably due to the electrostatic association between the positive charge of the polyplexes and the negative charge of the plasma membrane. If the disulfide linkages were reduced prior to uptake by cells, a higher percentage of the PEG-SS-P[Asp(DET)] micelles would be taken up than the PEG-P[Asp(DET)] micelles. In contrast, the cellular uptakes of PEG-P[Asp(DET)] and PEG-SS-P[Asp(DET)] micelles are equivalent, suggesting that the

(31) Kataoka, K.; Harada, A.; Nagasaki, Y. *Adv. Drug Delivery Rev.* **2001**, *47*, 113–131.

(32) Kwok, K. Y.; McKenzie, D. L.; Evers, D. L.; Rice, K. G. *J. Pharm. Sci.* **1999**, *88*, 996–1003.

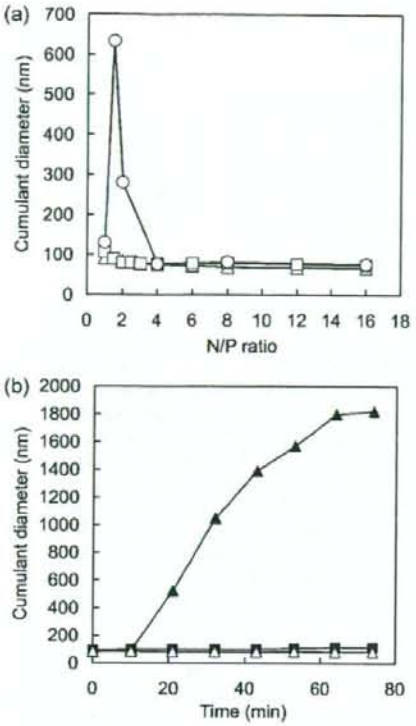


*Figure 4.* (a) Size of the polyplexes from PEG-SS-P[Asp(DET)] (△), PEG-P[Asp(DET)] (□), and P[Asp(DET)] (○). (b) Time-dependent change of the size of PEG-SS-P[Asp(DET)] polyplex micelles at $N/P = 2$ with 10 mM DTT (▲) and with 10 $\mu$M DTT (△), and PEG-P[Asp(DET)] polyplex micelles with 10 mM DTT (■).

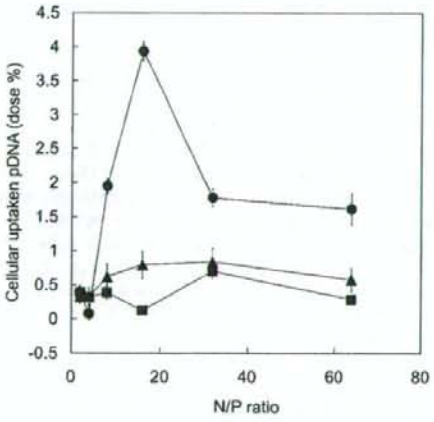


*Figure 5.* Cellular uptake of pDNA complexed with catiomers; PEG-SS-P[Asp(DET)] (▲), PEG-P[Asp(DET)] (■), and P[Asp(DET)] (●). $^{32}$P-labeled pDNA polyplexes were incubated with HeLa cells in DMEM containing 10% FBS at 37 °C for 6 h. The amount of internalized pDNA is represented as a percentage for the dosed pDNA (1 $\mu$g/well).

PEG-SS-P[Asp(DET)] micelles maintain their PEG palisade structure under normal culture conditions for at least 6 h. Note

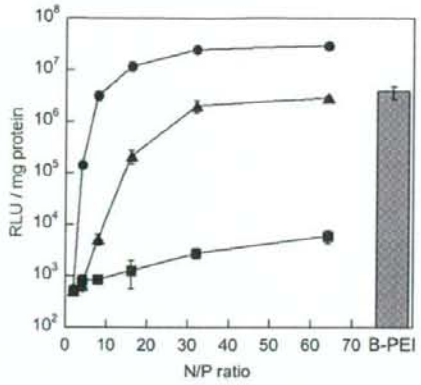


*Figure 6.* In vitro transfection of the luciferase gene into HeLa cells by polyplexes from PEG-SS-P[Asp(DET)] (▲), PEG-P[Asp(DET)] (■), and P[Asp(DET)] (●) with varying *N/P* ratios. Branched polyethyleneimine (B-PEI, 25 kDa) at $N/P = 32$ was shown as a control (gray bar). The cells were incubated with each polyplex in DMEM containing 10% FBS for 6 h, followed by incubation for a further 42 h in the absence of the polyplexes. Transfection is reported in relative light units (RLU) per mg of protein.

that there is a decrease in cellular uptake of the P[Asp(DET)] polyplexes with $N/P \geq 32$. This may be due to inhibition of uptake by free catiomers which are not associated with the polyplexes.

**In Vitro Transfection Efficiency and Cytotoxicity.** The in vitro transfection efficiency of these polyplexes with HeLa cells was assessed using a luciferase assay. Based on the cellular uptake study, cells were incubated with the polyplexes for 6 h, followed by a 42 h incubation after medium replacement. As shown in Figure 6, PEG-SS-P[Asp(DET)] polyplex micelles showed 2–3 orders of magnitude higher transfection efficiency than the PEG-P[Asp(DET)] polyplex micelles at $N/P \geq 16$, which is comparable to branched polyethyleneimine (B-PEI, 25 kDa). It is surprising that the introduction of disulfide linkages to the block catiomers remarkably increased the transfection efficiency, though the efficiency was somewhat less than P[Asp(DET)] polyplexes. Low cytotoxicity together with high transfection efficiency is an extremely important aspect for nonviral gene vectors. The cytotoxicity of the polyplexes was evaluated with the same cell culture procedure as the transfection, followed by the CellTiter-Glo luminescent cell viability assay. Polyplex micelles from PEG-SS-P[Asp(DET)], PEG-P[Asp(DET)], and P[Asp(DET)] polyplexes showed more than 90% cell viability in all *N/P* ratios tested in this study, while B-PEI polyplexes induced a significant decrease in cell viability (~40%) at $N/P = 64$ (Figure S5). A similar tendency was observed at lower *N/P* as well in the case of longer incubation times and higher doses (data not shown). These results indicate that P[Asp(DET)] and the block catiomers would be desirable as in vivo gene vectors due to their high transfection efficiency as well as low toxicity.

**Mechanism of the High Transfection Efficiency of PEG-SS-P[Asp(DET)] Micelles.** It is important to understand where the disulfide linkages of the PEG-SS-P[Asp(DET)] polyplex micelles are cleaved inside the cell. Therefore, the time-dependent profile of transfection efficiency was monitored with AB-2550 Kronos Dio (ATTO Co. Ltd., Tokyo, Japan), which is a luminometer incorporated into a small $CO_2$ incubator, allowing continuous measurement of bioluminescence by transfected

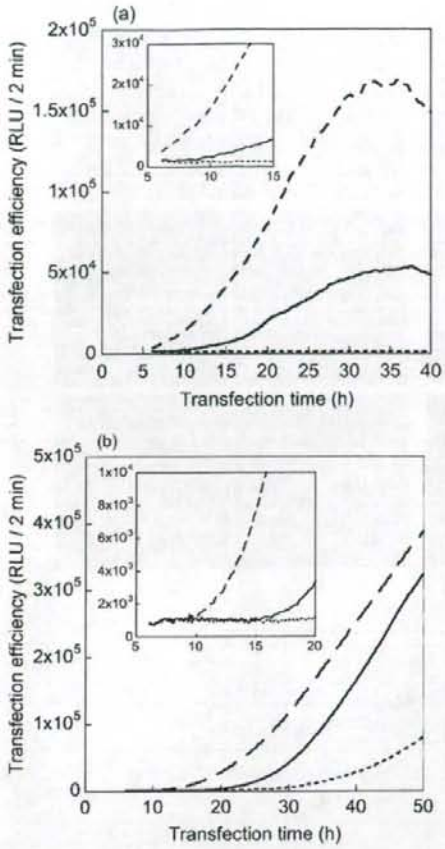


*Figure 7.* Time-dependent profiles of transfection efficiency against HeLa cells (a) and 293T cells (b) induced by PEG-SS-P[Asp(DET)] (solid line), PEG-P[Asp(DET)] (dotted line), and P[Asp(DET)] (dashed line) polyplexes at $N/P = 32$. The cells were incubated with each polyplex in DMEM containing 10% FBS for 6 h, followed by incubation in DMEM containing 10% FBS and 100 $\mu$M D-luciferin in the absence of polyplexes. The time shown in the $x$-axis started from the addition of polyplex solutions and the measurement started from 6 h. The inserts are expanded figures from 5 to 15 h (a) and from 5 to 20 h (b).

cells. After HeLa cells were incubated with the polyplexes for 6 h, the medium modified to include luciferin was used to culture the cells and bioluminescence from expressed luciferase was monitored at 20 min intervals. As shown in Figure 7a, the gene expression induced by P[Asp(DET)] polyplexes started to be observed immediately after the medium replacement (at 6 h), while the expression by PEG-SS-P[Asp(DET)] micelles started at 11 h and increased remarkably after 16 h. A similar tendency of delayed expression with PEG-SS-P[Asp(DET)] micelle carriers compared with P[Asp(DET)] polyplexes was observed with 293T cells as well (Figure 7b). The reason of the delayed expression of PEG-SS-P[Asp(DET)] micelles is presumably related to the process of the disulfide reduction inside the cell. In addition, clear expression by PEG-SS-P[Asp(DET)] micelles in 293T cells was observed 10 h earlier than PEG-P[Asp(DET)] micelles, probably due to the detachment of PEG chains. These results indicate that PEG-SS-P[Asp(DET)] micelles could regulate the onset of the gene expression, which is a significantly attractive characteristic in this system.

In order to gain more insight into the relationship between the cleavage of disulfide linkages and transfection efficiency, intracellular trafficking of pDNA in the micelles was observed with a confocal laser scanning microscope (CLSM), using PEG-SS-P[Asp(DET)] polyplex micelles with Cy5-labeled pDNA (red) at $N/P = 32$. LysoTracker (green) was used as an endo/lysosomal marker. As shown in Figure 8a, Cy5-pDNA of the polyplex micelles from PEG-P[Asp(DET)] and PEG-SS-P[Asp(DET)] associates to the plasma membrane 6 h after transfection, whereas the red fluorescence from P[Asp(DET)] polyplexes seemed to spread out from the green fluorescence of LysoTracker even at 6 h, indicating fast endosomal escape. This result would correspond to the transfection profile (Figure 7a) where transfection by P[Asp(DET)] polyplexes is observed starting at 6 h. Figure 8b shows CLSM images after 6 h of incubation with the polyplex and 6 h postincubation in the absence of polyplexes, corresponding to the time when a gene expression by PEG-SS-P[Asp(DET)] micelles started (12 h in Figure 7a). In these images, the pDNA of PEG-P[Asp(DET)] micelles is colocalized and sequestered in the endo/lysosome, resulting in the absence of expression in Figure 7a. On the other hand, the pDNA of PEG-SS-P[Asp(DET)] micelles spread out from LysoTracker, indicating that the PEG-SS-P[Asp(DET)] micelles that escaped from the endosome would be capable of inducing gene expression. In the case of P[Asp(DET)] polyplexes, pDNA spread out from endo/lysosome increased remarkably. Time-dependent colocalization of pDNA in the endo/lysosomes was quantified and is shown in Figure 8c. PEG-P[Asp(DET)] micelles exhibited high colocalization even after 2 days, while less colocalization was observed in the PEG-SS-P[Asp(DET)] system, suggesting a more effective endosomal escape. A similar localization profile of pDNA in the PEG-SS-P[Asp(DET)] system was observed in 293T cells (Figure S6). Considering the transfection profile as well as CLMS images (Figure 7 and 8), it is likely that cleavage of the disulfide linkages of PEG-SS-P[Asp(DET)] micelles occurs in the endocytic pathway, resulting in effective endosomal escape probably due to interaction between the exposed polycation segments and endosomal membrane, and/or increased osmotic pressure in the endosome induced by detached PEG chains. As a result, the gene expression onset of PEG-SS-P[Asp(DET)] micelles was intermediate when compared with P[Asp(DET)] polyplexes and PEG-P[Asp(DET)] micelles. There is an issue that disulfide reduction in the endosome would be disfavored due to the low GSH concentration as well as the acidic environment inducing protonation of thiol groups and decreased reactivity of thiol−disulfide oxidoreductase (e.g., PDI, thioredoxin, etc.) because these enzymes typically exhibit optimal activity around neutral pH. Nevertheless, Low et al. directly observed images of disulfide cleavage with FRET technology using folate−SS−rhodamine conjugates.[33] In addition, calcein-loaded polymersome formed from a PEG-SS-poly(propylene sulfide) block copolymer showed the rapid release of calcein inside the endosome due to the disulfide reduction, facilitating endosomal rupture.[34] In the case of the PEG-SS-P[Asp(DET)] system, considering the increased endosomal escape, not all PEG chains but a substantial fraction of them are assumed to be detached

(33) Yang, J.; Chen, H.; Vlahov, I. R.; Cheng, J.-X.; Low, P. S. *Proc. Natl. Acad. Sci. U.S.A.* **2006**, *103*, 13872–13877.
(34) Cerritelli, S.; Velluto, D.; Hubbell, J. A. *Biomacromolecules* **2007**, *8*, 1966–1972.

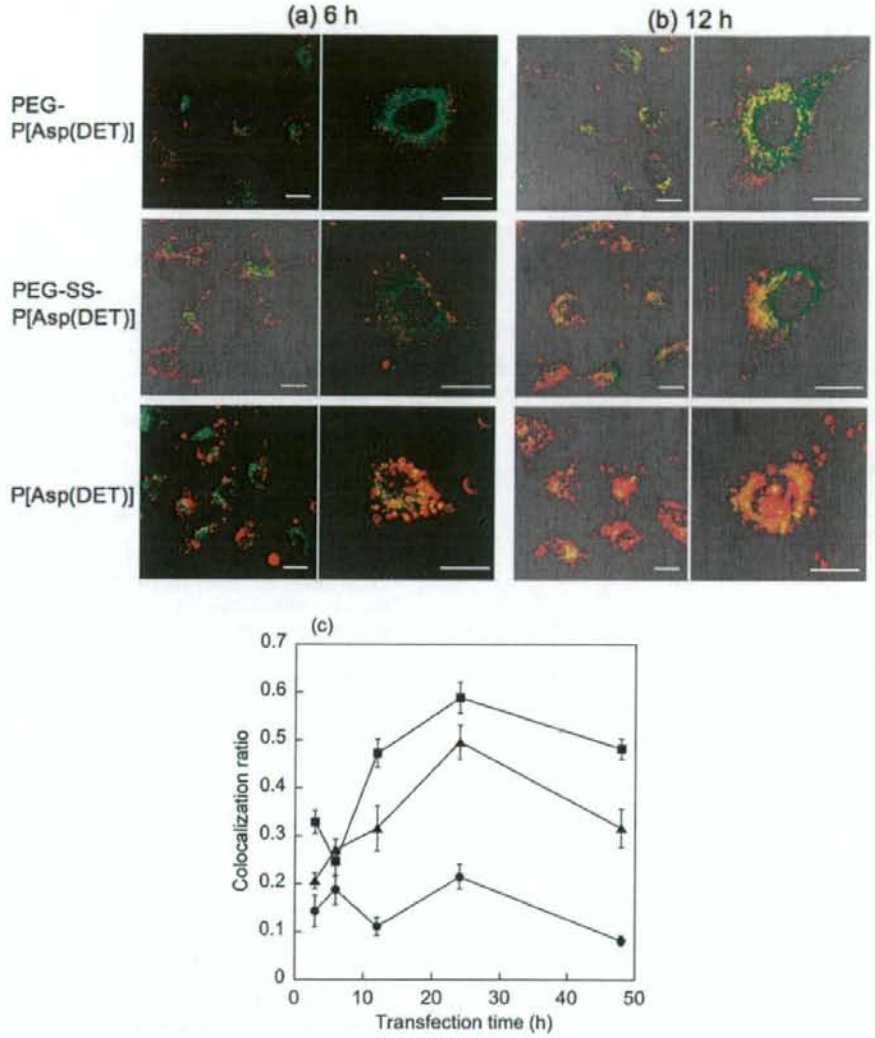


***Figure 8.*** (a, b) Intracellular distribution of pDNA challenged by PEG-P[Asp(DET)] and PEG-SS-P[Asp(DET)] micelles, and P[Asp(DET)] polyplexes at $N/P = 32$. The complexes loaded with Cy5-labeled pDNA (red) were incubated with HeLa cells for 6 h, followed by incubation in the absence of polyplexes. The CLSM observation was performed 6 h (a) and 12 h (b) after transfection, using a 63× objective. The acidic late endosome and lysosome were stained with LysoTracker Green (green). The scale bar represents 20 $\mu$m. (c) Quantitative results of colocalization profile of Cy5-labeled pDNA in late endosome and lysosome transfected by PEG-P[Asp(DET)] (■), PEG-SS-P[Asp(DET)] (▲), and P[Asp(DET)] (●) polyplexes.

in the endocytic pathway as a result of disulfide reduction. In the future, further mechanistic investigations of the disulfide cleavage will be performed to reveal a detailed relationship between PEG detachment and gene transfection efficiency, contributing to establishing the design criteria for smart polyplex micelles useful for in vivo transfection studies.

## Conclusion

We newly synthesized a disulfide-linked block catiomer, PEG-SS-P[Asp(DET)], to develop a PEG detachable polyplex micelle sensitive to an intracellular reducing environment. This micelle showed several orders of magnitude higher gene transfection efficiency than a micelle without disulfide linkages in spite of the similar level of their cellular uptakes. Moreover, gene expression induced by the PEG-SS-P[Asp(DET)] micelle started between the expression onsets of the P[Asp(DET)] polyplex and PEG-P[Asp(DET)] micelle, indicating that the PEG-SS-P[Asp(DET)] micelle could regulate the onset of the gene expression. CLSM images revealed that this transfection behavior of the PEG-SS-P[Asp(DET)] micelle could be explained by effective endosomal escape due to the PEG detachment in the endosome. As this micelle overcame the PEG dilemma, it would be highly promising for in vivo application to exert spatio-temporal regulated transfection with minimal cytotoxicity.

**Acknowledgment.** The authors acknowledge Mr. Shigeto Fukushima, the University of Tokyo, for his advice about polymer synthesis. This study was financially supported by the Core Research for Evolutional Science and Technology (CREST) from the Japan Science and Technology Agency (JST) and also by a grant for the 21st Century COE Program "Human-Friendly Materials based on Chemistry" from the Ministry of Education, Culture, Sports, Science and Technology of Japan (MEXT). S.T. would like to express his special gratitude for the scholarship from the Asahi Glass Scholarship Foundation.

**Supporting Information Available:** $^1$H NMR spectra and GPC charts of PEG-SS-$NH_2$, PEG-SS-PBLA and PEG-SS-P[Asp-(DET)], ζ-potential measurements, cytotoxicity study, and CLSM images of 293T cells. These materials are available free of charge via the Internet at http://pubs.acs.org.

JA800336V